e-Polymers **2004**, no. 064.

http://www.e-polymers.org
ISSN 1618-7229

Morphology and phase behaviour of poly(propylene oxide) containing copoly(ether ester)s

Ronald F. M. Lange [1,2] *, *Wouter Gabrielse* [1]

[1] DSM Research, P.O. Box 18, 6160 MD Geleen, The Netherlands

[2] Present address: BASF, E-MEE/J550, 67056 Ludwigshafen;
Fax +49 621 60 43205; ronald.lange@basf-ag.de

(Received: August 3, 2004; published: October 9, 2004)

Abstract: The morphology and phase behaviour of six different copoly(ether ester) elastomers, based on poly(butylene terephthalate) (PBT) hard blocks and poly-(ethylene oxide)-*block*-poly(propylene oxide)-*block*-poly(ethylene oxide) (PEO-*b*-PPO-*b*-PEO) soft blocks, differing in soft-block content and molecular weight of the soft block, have been investigated using various analytical techniques such as DSC, dynamic mechanical thermal analysis, dielectric spectroscopy, ^{13}C CP-MAS NMR, AFM, TEM, and optical microscopy. The PBT blocks were found to crystallize in lamellar structures that form a continuous highly interconnected architecture. No crystalline regions for the PEO-*b*-PPO-*b*-PEO triblock could be observed, whereas no indications of a separate pure amorphous PBT phase were found. It is further shown that the amorphous phase is not a homogeneous mixture of amorphous PBT and soft segments. Based on the combined results of the analytical techniques used it is concluded that the PPO segments form an almost pure amorphous phase, whereas the PEO segments form a mixed phase with amorphous PBT. It is believed that the presence of this pure amorphous PPO phase provides the PEO-*b*-PPO-*b*-PEO containing copoly(ether ester)s with their excellent cold-temperature properties.

Introduction

Thermoplastic elastomers or TPE's are able to combine their elastic properties with the broadly used thermoplastic processing due to the formation of a phase-separated morphology [1]. In polyester-based thermoplastic elastomers or TPE-E's, this phase separation is obtained by the crystallisation of the hard polyester phase in a soft amorphous polyether-rich phase [1,2]. The aim in these TPE-E's is to control the formation of a well-defined two-phase morphology so that the elastomeric properties can be fully exploited. This control can be achieved by studying the relation between the molecular structure, the morphology, and the resulting mechanical properties. Industrially, three TPE-E grades are frequently used, in which the crystalline hard segment is poly(butylene terephthalate) (PBT), and the amorphous soft segment consist of poly(ethylene oxide) (PEO), poly(tetramethylene oxide) (PTMO), or poly-(ethylene oxide)-*block*-poly(propylene oxide)-*block*-poly(ethylene oxide) (PEO-*b*-PPO-*b*-PEO). The PEO-based TPE-E is used in, *e.g.*, breathable (outdoor) clothing, whereas the other two grades are frequently encountered in highly demanding automotive applications like, *e.g.*, constant velocity joint boots. The morphology and

phase separation of the PEO and PTMO containing copoly(ether ester)s has been studied in detail [1-15]. In the molten state a homogeneous polymer melt is obtained from which, upon cooling, the PBT starts to crystallise and induces the phase separation [3-5]. The crystalline structure is lamellar (although dendritic and shish kebab structures have also been reported) [6-11], and a crystalline superstructure (spherulites) can be formed depending on the crystallization conditions [12]. Within the composition range studied, most authors conclude that both the crystalline and amorphous phase of the PTMO-based copoly(ether ester)s are co-continuous [13-16]. The co-continuous PBT phase is reflected in the relative high modulus of the materials. The amorphous phase has long been considered to be homogeneous, but more recent solid-state NMR studies showed that the amorphous phase is separated in a mixed amorphous PBT-PTMO phase and a relatively pure PTMO phase [17].

Extremely phase-separated PBT-based copoly(ether ester)s containing a highly apolar hydrogenated polybutadiene (PEB) soft block have also been reported [18-20]. The successful synthesis of this kind of copoly(ether ester)s was possible by using a PEO-*b*-PEB-*b*-PEO soft block, in which the PEO blocks act as a compatibiliser during the synthesis. The morphology in this kind of copoly(ether ester)s is induced by the crystallisation of the PBT from a phase-separated polymer melt, as shown using dynamic shear experiments in combination with small-angle X-ray scattering [19]. A disperse crystalline PBT phase was obtained next to an amorphous phase that consisted of a pure amorphous PEB and PBT phase, a relatively pure PEO phase and a mixed amorphous PBT-PEO phase [20]. Hysteresis measurements demonstrated that the PEB-containing copoly(ether ester)s showed a significantly improved elastic behaviour compared to PTMO-based copoly(ether ester)s.

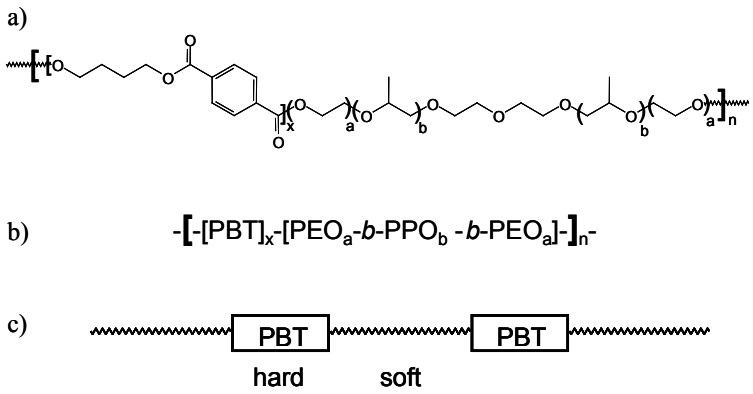

Fig. 1. Structure of PBT and PEO-*b*-PPO-*b*-PEO based copoly(ether ester)s: a) chemical structure; b) simplified structure; c) schematic structure

No detailed information is available concerning the morphology of the PEO-*b*-PPO-*b*-PEO based copoly(ether ester)s. This class of copoly(ether ester)s is highly interesting since they combine industrial availability with the interesting phase behaviour of 'academic' PEO-*b*-PEB-*b*-PEO containing TPE-E's. Here we present a detailed study concerning the morphology and phase behaviour of copoly(ether ester) elastomers, based on PBT hard blocks and PEO-*b*-PPO-*b*-PEO soft blocks. A wide compositional range using six different grades differing systematically in soft block content and molecular weight of the soft block has been investigated to provide a more general understanding of the morphology of the copoly(ether ester)s. The phase behaviour and microstructure of these model systems was characterized in

detail by a number of experimental techniques including optical microscopy, atomic force microscopy (AFM), transmission electron microscopy (TEM), differential scanning calorimetry (DSC), dynamic mechanical thermal analysis (DMTA), dielectric spectroscopy (DIES), and ^{13}C CP-MAS NMR, covering length scales of µm to Å. Based on the obtained results a refined structural model is proposed, which should help to provide a better understanding of the relation between molecular structure, morphology and mechanical properties.

Results and discussion

The morphology of the copoly(ether ester)s on micrometer scale can be envisaged by optical microscopy. An optical micrograph of P2200/55 shows well developed spherulites possessing a diameter of about 10 µm, as is depicted in Fig. 2. A more detailed picture of the lamellar structures within the spherulites is obtained by transmission electron microscopy. TEM pictures of P1700/25, P2200/25 and P2200/55 are shown in Fig. 3 (sample coding is given in the Exptl. part). The soft PEO-*b*-PPO-*b*-PEO domains absorb the staining agent and are visible as black regions, whereas the white regions represent the hard, crystalline PBT domains. The TEM micrographs clearly indicate that the samples possess at least a two-phase morphology. Typical domain sizes of the soft amorphous regions are about 20 nm.

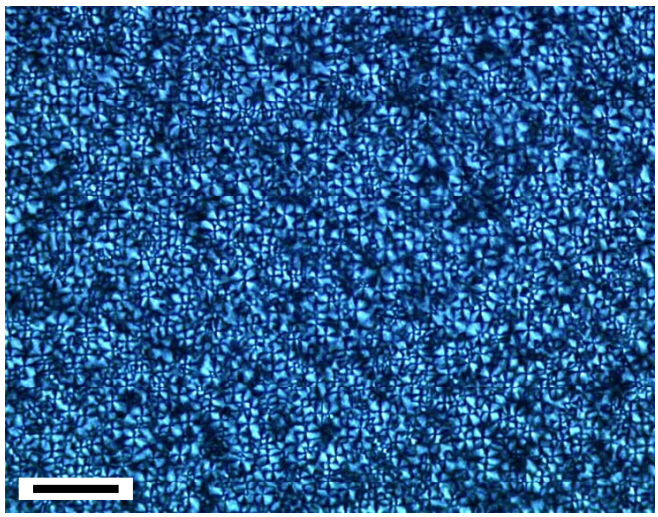

Fig. 2. Optical micrograph of a copoly(ether ester). The scale bar represents 50 µm

The two-phase, lamellar morphology is also clearly revealed by AFM (see Fig. 4). In the AFM micrographs the continuous lamellar crystalline structure, which is more pronounced for P2200/25, is clearly visible. This continuous structure is also reflected by a high initial modulus in the stress-strain analysis [17,20].

To investigate the phase behaviour of the different copoly(ether ester)s, DSC and DMTA measurements were performed. In Fig. 5, the second heating and cooling curves of the DSC measurements of the copoly(ether ester) samples are depicted. At about -60°C the glass transition of the PEO-*b*-PPO-*b*-PEO soft block, and above 200°C the melting endotherms of the PBT hard blocks are observed. The multiple melting peaks are due to recrystallisation and melting processes, as was proven by DSC experiments performed at various scanning rates. Before melting, a small endothermic effect is observed at a temperature, which coincides with the

crystallization temperature of the compound. This melting and recrystallisation behaviour is common for polyesters [21].

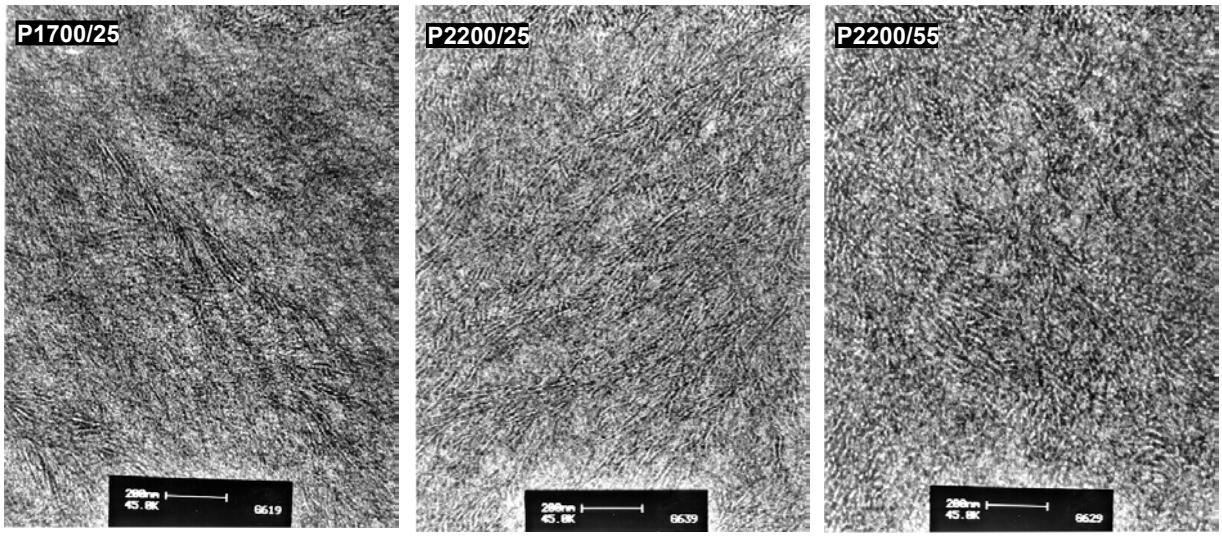

Fig. 3. Transmission electron micrographs of a) P1700/25, b) P2200/25 and c) P2200/55. The pictures have the same scaling factor with the scale bar at the bottom of the picture representing 200 nm (sample coding is given in the Exptl. part)

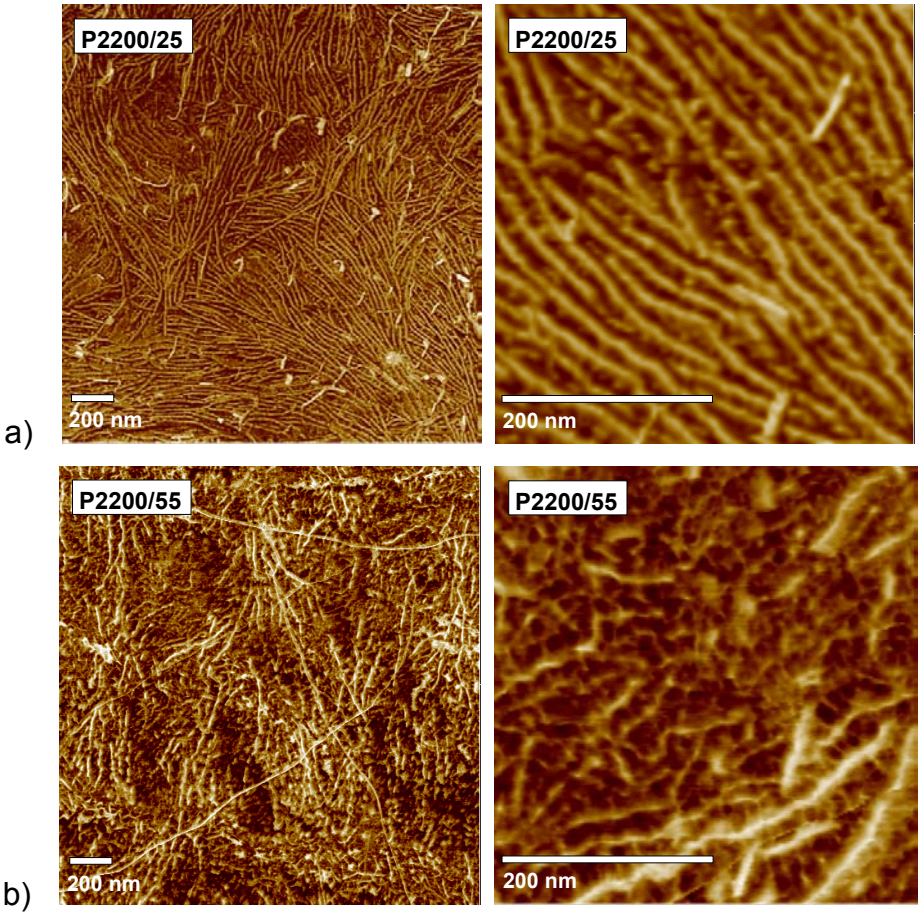

Fig. 4. AFM micrographs of a) P2200/25 and b) P2200/55. The scale bar at the bottom of the picture represents 200 nm

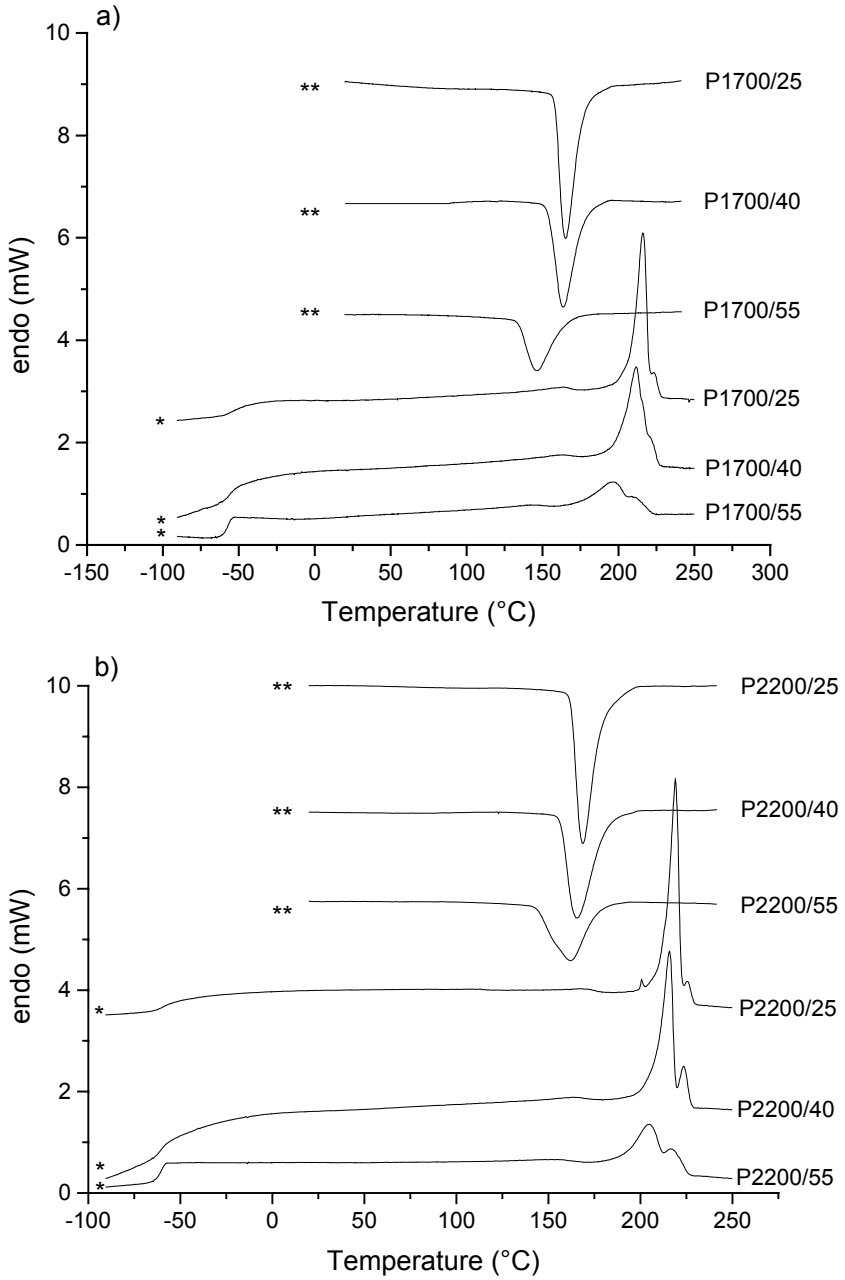

Fig. 5. Differential scanning calorimetry (DSC) analysis of a) P1700/25, P1700/40 and P1700/55, and b) P2200/25, P2200/40 and P2200/55. The second heating (*) and cooling (**) curves, recorded using a heating rate of 10°C/min, are depicted

Comparing the different copoly(ether ester) samples, it is observed that the melting temperature and crystallization temperature of PBT increases with increasing block length (see Tab. 1 in the Exptl. part). These results, which are consistent with the results obtained for PTMO- and PEB-containing copoly(ether ester)s, suggest that crystallite size and perfection increase with increasing block length. For all samples a glass transition of the PEO-*b*-PPO-*b*-PEO soft block is observed at about -55 to -60°C. It is noticeable that this T_g is not significantly shifted with composition. In the pure PEO-*b*-PPO-*b*-PEO diol, which is phase-separated, a T_g at -60°C is observed, which is attributed to the PPO phase, followed by a crystallization and melting peak of the PEO phase at about -40 and 0°C, respectively. This is not observed in the PEO-*b*-PPO-*b*-PEO containing TPE-E's, indicating that there is no distinct PEO

phase. Since the crystallinity of homo-PBT is about 45%, amorphous PBT is present in the samples. However, no glass transition of an amorphous PBT phase at about 50°C could be detected in the second heating run.

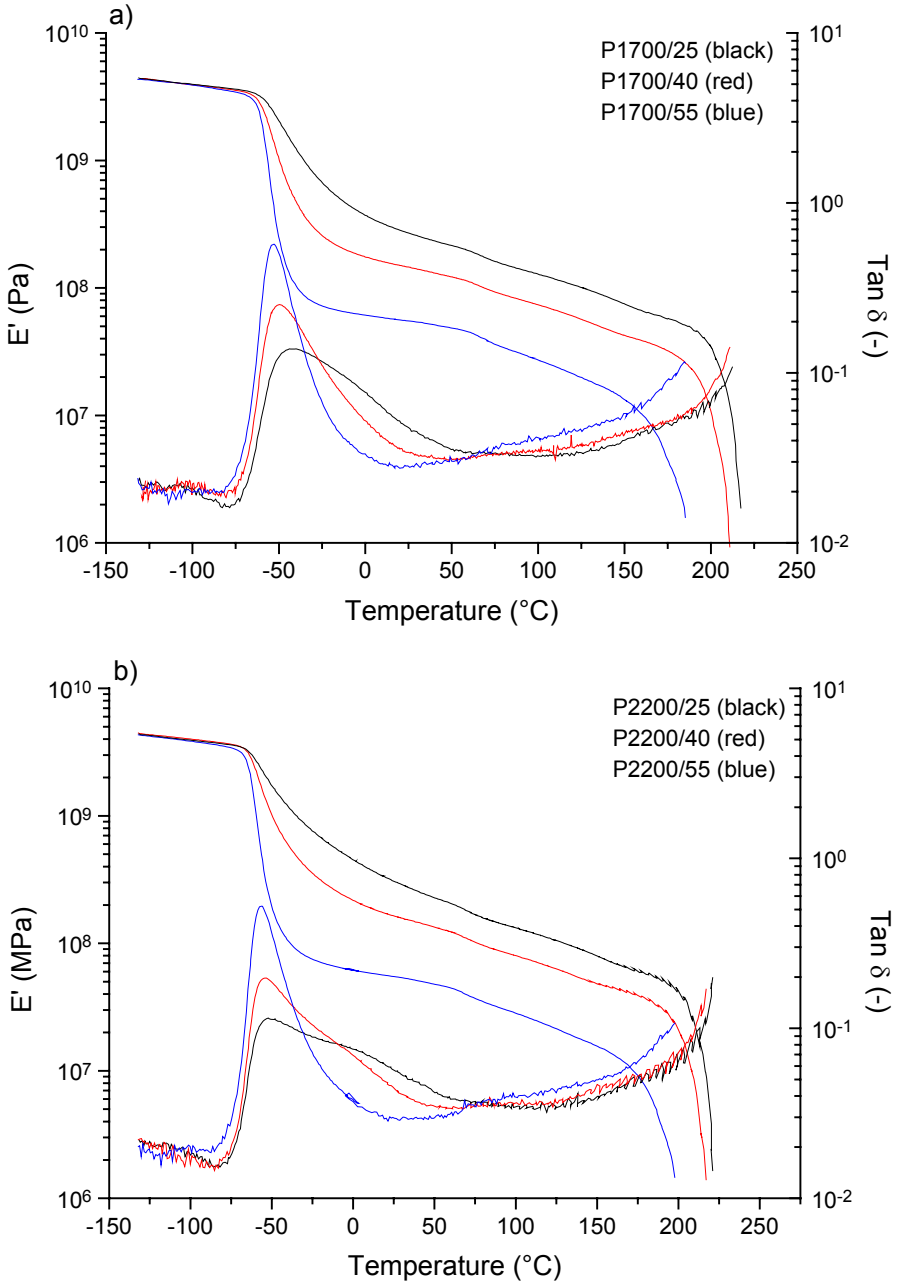

Fig. 6. Dynamic mechanical thermal analysis (DMTA) of a) P1700/25, P1700/40 and P1700/55, and b) P2200/25, P2200/40 and P2200/55, showing the temperature dependency of the tensile modulus and tan δ. The measurements were recorded using a frequency of 1 Hz

The DMTA curves of the melt-pressed copoly(ether ester) samples, showing *E'* and tan δ versus temperature, are depicted in Fig. 6. Basically the same transitions are observed as with DSC analysis. Heating the sample from -150°C, the glass transition temperature (T_g) of the PEO-*b*-PPO-*b*-PEO soft block is seen at about -60°C. Above this T_g an extended rubber plateau is observed which is typical of copoly(ether ester)-

like elastomeric materials. Finally, above about 150°C the melting of the PBT hard domains starts, resulting in a dramatic decrease of the modulus. In the rubber plateau, two minor drops in the modulus are observed at about 60°C and at temperatures of about 145 to 170°C. These effects are probably related to melting and/or recrystallization of small and/or imperfect PBT crystals. The effect at 60°C is also observed in the first heating curves of a DSC measurement (not shown here). The small drop in modulus at about 145 to 170°C, which coincides with the crystallization temperatures of the materials (see Tab. 1), is also observed as a small endothermic effect in the second DSC heating curves. In analogy with the DSC measurements, no transitions due to the melting of the PEO blocks in the PEO-*b*-PPO-*b*-PEO soft block are observed.

Comparing the different copoly(ether ester) samples, it is seen that with increasing soft content a decrease of the tensile modulus at room temperature and a decrease of the melting point is obtained. The samples containing a relatively high amount of soft block show, in analogy with DSC measurements, a more defined T_g with a slightly asymmetric tan δ peak. The asymmetric tan δ maximum becomes more pronounced for the samples containing a relatively low amount of soft block. In fact, two separate T_g's can be distinguished. The first T_g, which is observed for all samples at about -60°C, does not change with composition, whereas the second T_g is shifted towards higher temperatures with decreasing soft content. The low T_g observed at -60°C, which is also observed for the pure PEO-*b*-PPO-*b*-PEO triblock, is attributed to a nearly pure PPO phase. The second T_g is attributed to a PBT-PEO mixed phase, which shifts to higher temperatures with increasing PBT content. These assignments are consistent with the comparable χ parameters between PEO and PBT ($\chi_{PEO\text{-}PBT}$ = 0.014) whereas the χ parameter between PPO and PBT is strongly different ($\chi_{PPO\text{-}PBT}$ = 0.168) [22]. Dielectric spectroscopy (DIES) data are in analogy with the results obtained using DMTA as is depicted in Tab. 1.

In summary, these results point to the following morphology for the PEO-*b*-PPO-*b*-PEO copoly(ether ester)s: a crystalline lamellar PBT phase, which is surrounded by an amorphous phase consisting of a mixed PEO-PBT phase and an almost pure PPO phase. In order to provide more evidence for this proposed morphology, ^{13}C CP-MAS NMR measurements were performed.

^{13}C CP-MAS NMR relaxation measurements were performed to investigate the microphase structure of PEO-*b*-PPO-*b*-PEO containing copoly(ether ester)s. Especially NMR relaxation studies are of interest, since changes in morphology are usually accompanied by changes in the molecular mobility, which are reflected in NMR relaxation times. Several NMR relaxation experiments were performed including variable contact time CP-MAS experiments, ^{13}C IRCP experiments and $T_{1\rho}(^1H)$ experiments.

A ^{13}C solid-state CP-MAS spectrum of P1700/55 is shown in Fig. 7. It is possible to distinguish between the OCH_2 and OCH resonances originating from PBT, PEO and PPO segments (60 - 80 ppm), which allows separate molecular mobility studies of the various blocks. To investigate the molecular mobility of the PEO and PPO segments, ^{13}C CP-MAS NMR spectra were recorded as a function of the contact time during cross-polarisation. For all samples a difference in line width at short and long cross-polarisation times is observed for the PEO-OCH_2 and the PPO-OCH and PPO-OCH_2 carbons at room temperature. As an example, Fig. 8 shows the ^{13}C spectra of P2200/55 at a short and a long mixing time of 200 µs and 30 ms, respectively. The difference in line-width at short and long mixing times already indicates that there is

heterogeneity in the molecular mobility of the PEO and PPO carbons in the amorphous phase.

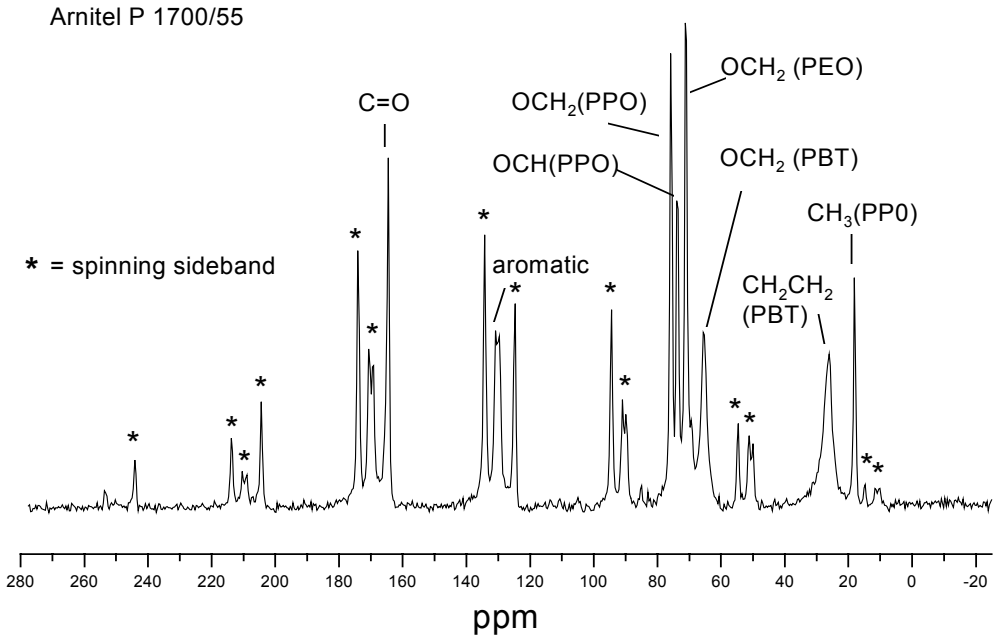

Fig. 7. NMR spectrum of P1700/55. Spinning speed 4 kHz, number of transients 2000, CP contact time 1 ms

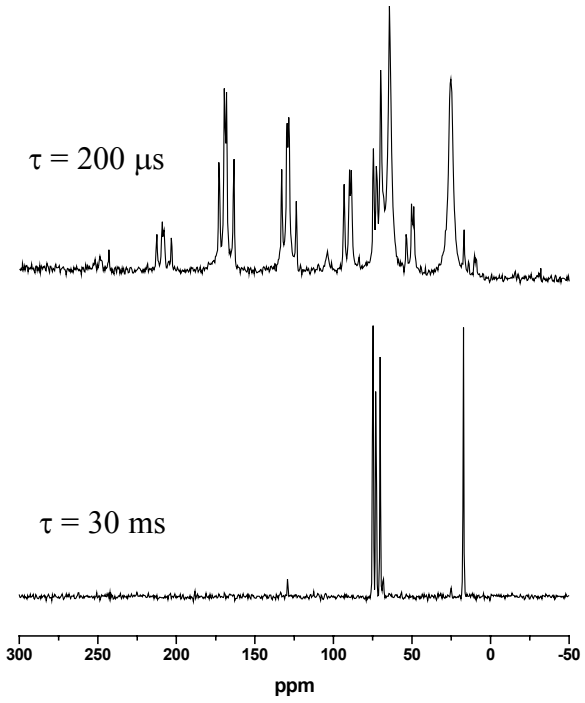

Fig. 8. ^{13}C CP-MAS spectra of P2200/55 at cross-polarisation times of 200 μs (giving information about relatively rigid phases) and 30 ms (giving information about highly mobile phases)

In order to provide clear evidence for the existence of overlapping narrow and broad PEO-OCH_2, PPO-OCH and PPO-OCH_2 resonances, ^{13}C inversion recovery cross-

polarization (IRCP) experiments were performed. Some decomposed spectra recorded in a ^{13}C IRCP experiment are shown in Fig. 9 for sample 1700/55. Curve fitting of these spectra shows that the OCH_2 resonances of PEO and the OCH and OCH_2 resonances of PPO are actually built up of two peaks.

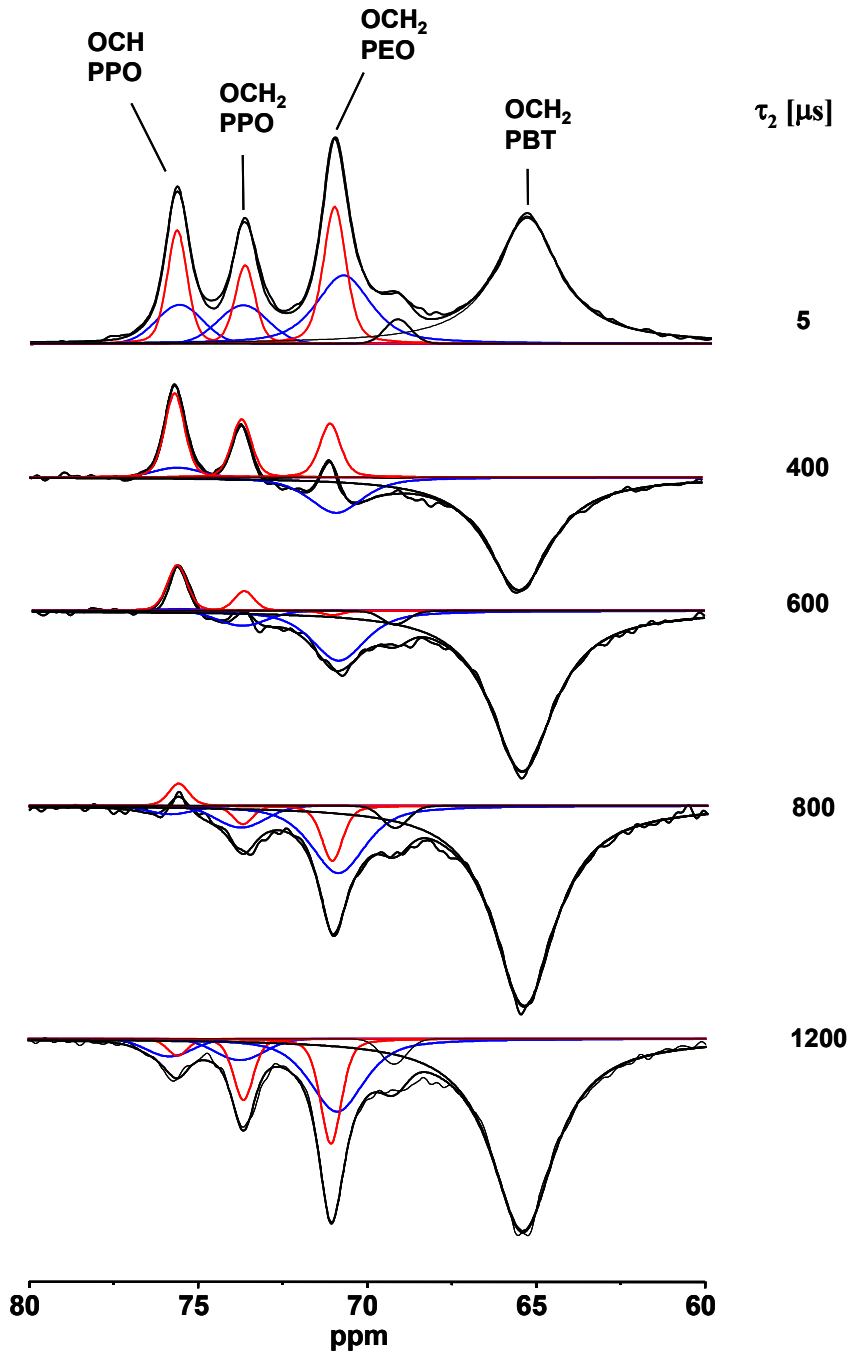

Fig. 9. ^{13}C IRCP deconvoluted spectra at various inversion times τ_2 of P1700/55

This effect seems to be more pronounced for PEO than for PPO. The splitting into two peaks becomes clear at the cross-over points. This is for the PEO-OCH_2 carbons at *c*. 400 μs, for the PPO-OCH_2 carbons at *c*. 600 μs, and for the OCH carbons of PPO at *c*. 800 μs. At this cross-over point a broad peak is observed (blue), which is already negative, and a narrow peak (red) that is still positive. The broad line can

unambiguously be assigned to carbons with more restricted mobility, whereas the narrow line can unambiguously attributed to carbons in a highly mobile (rubber-like) phase. Only a small difference in chemical shift (< *c*. 0.1 ppm) between both peaks can be detected, which reflects their different surroundings.

The splitting of the observed resonances into two peaks provides strong evidence for a microphase separation within the amorphous phase into a highly mobile phase that mainly consists of PPO segments and a phase with more restricted mobility, probably due to mixing of PEO segments with amorphous PBT. This suggestion is, next to the DSC and DMTA results, supported by $T_{1\rho}(^1H)$ spin diffusion experiments as discussed below.

Opposed to the above-described CP-MAS and IRCP experiments, where information is obtained about very local motions of individual groups, $T_{1\rho}(^1H)$ experiments give, due to the averaging effect of proton spin diffusion, information about domains with different mobility in the nanometer range. In addition, these $T_{1\rho}(^1H)$ experiments provide information about the miscibility of chemically different segments. It is noted that the $T_{1\rho}(^1H)$ decay was measured from the decay of carbons attached to them by using cross-polarisation. The integral intensities of the various peaks were determined as a function of the decay time. These data are plotted in Fig. 10.

The samples P2200/55 and P1700/55 show a bi-exponential decay with different slopes for PEO, PPO and PBT. This bi-exponential decay indicates the presence of different domains with different mobility. These domains are considered to have dimensions larger than 20 - 50 Å. For PBT, the fast decaying component is attributed to PBT in the amorphous phase, and the slower decaying component is attributed to PBT in the crystalline phase. For PEO and PPO the slow decaying component is attributed to soft segments with more restricted mobility (mixed with PBT), whereas the fast decaying component is due to soft segments in a highly mobile rubbery phase (no PBT present). These assignments are based on line-width considerations and are in agreement with previous assignments for PTMO- and PEB-based copoly(ether ester)s [17,20]. Obviously the longer $T_{1\rho}(^1H)$ relaxation times of PEO and PPO are quite similar, which indicates molecular mixing of both segments in the mobile phase. In contrast, differences are observed for the slow relaxing component, which means that the PEO and PPO segments are demixed to some extent. Since the short relaxation times for PEO and of PBT are similar, we conclude that mainly the PEO segments are mixed with amorphous PBT and that PPO forms an almost pure mobile rubbery phase. This is in agreement with the above-described DSC and DMTA measurements.

The samples possessing a relatively low soft-block concentration (P2200/25 and P1700/25) show a mono-exponential $T_{1\rho}(^1H)$ decay at room temperature with similar decay rates for PBT, PEO and PPO. This would indicate that there is strong mixing of these segments in the amorphous phase. However, DMTA measurements of these samples show an asymmetric peak in the tan δ curve where two T_g's can be resolved, a low T_g at about -60°C and a second T_g at about 0°C (see Fig. 6). This means that at least two amorphous phases must be present, which differ in composition. These two phases were not revealed by $T_{1\rho}(^1H)$ measurements at room temperature. Normally, the T_g as detected by NMR, which is sensitive to motions in the kHz range, is shifted about 50°C to higher temperatures compared to a T_g as determined with DMTA, which is sensitive to motions in the Hz range. Therefore, we recorded a $T_{1\rho}(^1H)$ experiment at 60°C (see Fig. 10b). At that temperature we clearly observe a bi-exponential decay, similar to that of the 'softer' P types. Again, the short $T_{1\rho}(^1H)$

value of PEO is similar to the short $T_{1\rho}(^1H)$ value of PBT, indicating substantial mixing of both components.

A

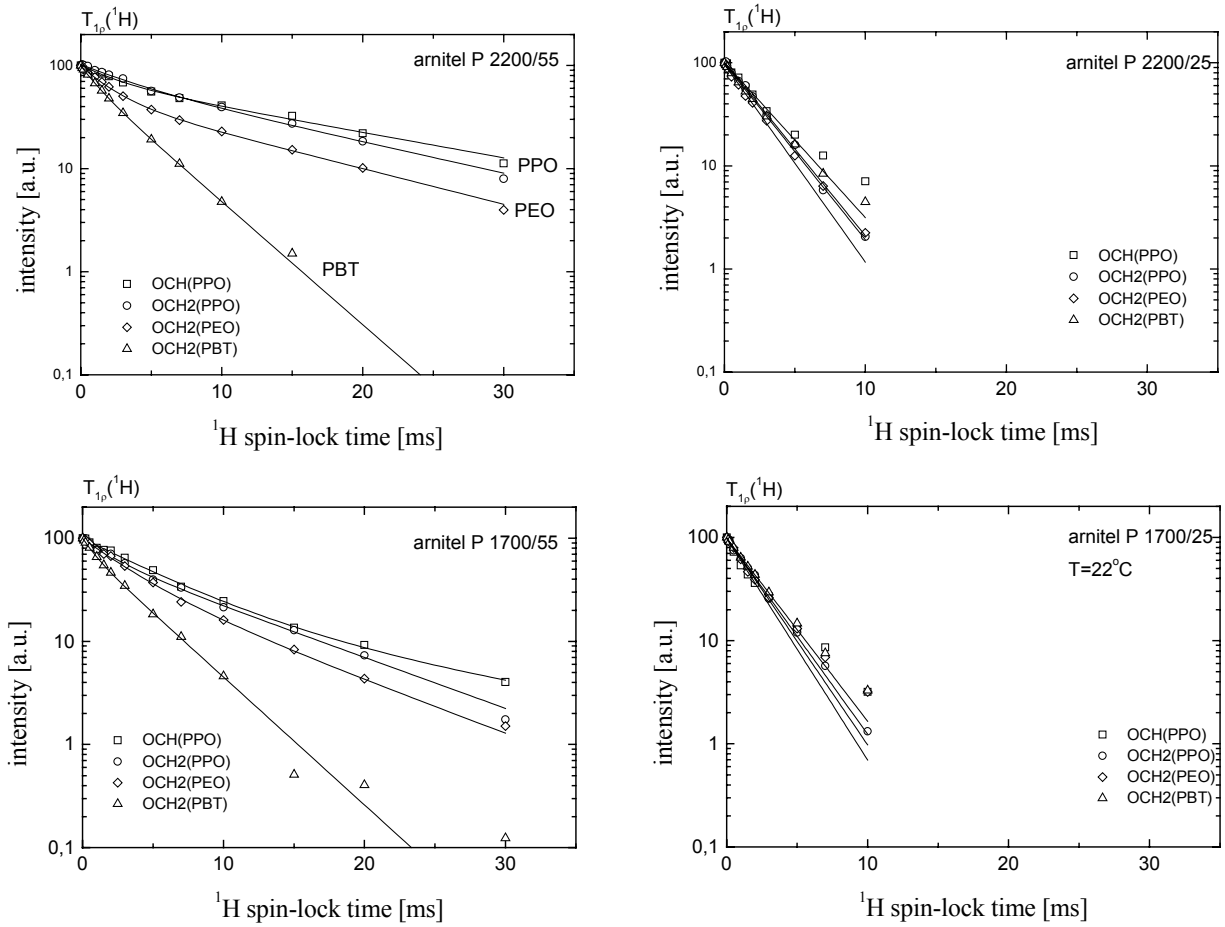

B

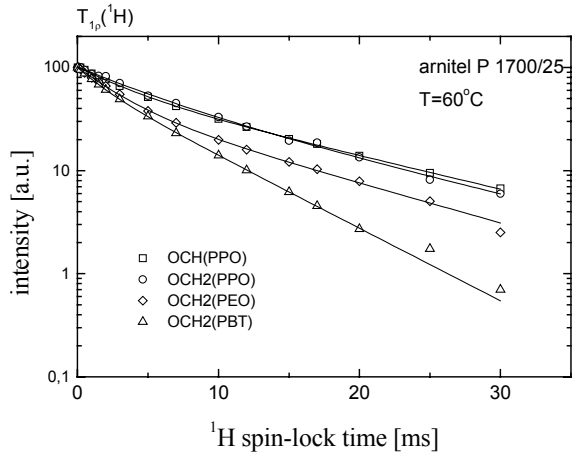

Fig. 10. A) $T_{1\rho}(^1H)$ relaxation decays for various copoly(ether ester) samples at room temperature, and B) relaxation decay for P1700/25 at 60°C

Conclusions

Various analytical techniques (DSC, DMTA, DIES, ^{13}C CP-MAS NMR, AFM, TEM, optical microscopy) have been applied to analyse the morphology and phase behaviour of six PEO-*b*-PPO-*b*-PEO based copoly(ether ester) grades, differing in soft block content and molecular weight of the soft block. The PBT blocks were found to crystallize in lamellar structures that form a continuous, highly interconnected

structure. No crystalline structures for the PEO-*b*-PPO-*b*-PEO triblock could be observed. In addition, it was shown that the amorphous phase is not a homogeneous mixture of amorphous PBT and soft segments. Based on the combined results of the analytical techniques used it is concluded that the PPO segments form an almost pure amorphous phase, whereas the PEO segments form a mixed phase with amorphous PBT. There are no indications for a separate pure amorphous PBT phase. We therefore propose the following three-phase model for PEO-*b*-PPO-*b*-PEO based copoly(ether ester)s as given below, including a crystalline PBT phase, a PEO/PBT mixed phase and an almost pure PPO phase. This proposed refined structural model of PEO-*b*-PPO-*b*-PEO based copoly(ether ester)s should help to provide a better understanding of the relation between molecular structure, morphology and mechanical properties.

Fig. 11. Proposed three-phase model for PEO-*b*-PPO-*b*-PEO based copoly(ether ester)s

Experimental part

The following compounds were prepared according to commercially used procedures [1,2,17]: copoly(ether ester) P1700/25, P1700/40, P1700/55, P2200/25, P2200/40 and P2200/55. The coding is as follows: P stands for the PEO-*b*-PPO-*b*-PEO soft block, 1700 and 2200 for the molecular weight (M_n) of the soft block, and 25, 40 and 55 for the soft-block content in wt.-%.

DSC measurements were performed on a Perkin-Elmer DSC-7, combined with a Perkin-Elmer CCA-7 liquid-nitrogen cooling accessory. DMTA measurements were recorded on a Rheometrics RSA2 using a constant frequency of 1 Hz and a heating rate of 5°C/min. Optical micrographs were obtained using a Leica DMRXP whereas TEM micrographs were obtained using a Philips CM200 electron microscope. The samples were stained for 48 h with a 1:1 mixture of a 2% aqueous solution of OsO_4 and a 20% aqueous solution of formaldehyde. AFM micrographs were recorded with a Nanoscope IIIa (Digital Instruments) in tapping mode from melt-pressed films using Teflon plates. ^{13}C CP-MAS NMR experiments were carried out with a Varian Unity 400 (400 MHz for ^{1}H) spectrometer using the 7 mm Jacobsen style VT CP/MAS probe. If not indicated, all NMR experiments were performed at room temperature. The 90° pulse width was 5 µs for protons and carbons. Adamantane was used as an external chemical shift reference (38.3 ppm for the methylene resonance relative to tetramethylsilane). All experiments were performed under magic angle spinning and high power decoupling conditions. A recycle time of 2 s was used in all cross-polarization experiments. ^{13}C Inversion recovery cross-polarization (IRCP) experiments were performed by applying a 180° phase shift on the proton spin-locking field. The cross-polarization time τ_1 was set to a fixed value of 1 ms. The 'inversion time' τ_2 was varied between 0.005 and 20 ms. ^{1}H $T_{1\rho}$ experiments were performed with a fixed cross-polarization time of 1 ms. The spin lock time on protons was varied between 10 µs and 30 ms. For the analysis of the NMR spectra, a self-written curve-fitting program was used.

Tab. 1. Summarized data for the PEO-*b*-PPO-*b*-PEO based copoly(ether ester) samples and the pure soft blocks obtained from the analytical methods used

TPE-E	PBT block length [a]	T_g DMTA [b]	T_g DIES [c]	T_g DSC [d]	ΔC_p soft block (PPO) in J/(g·°C)	T_m PBT DSC [d]	ΔH PBT in J/g	% PBT cryst. DSC [e]	T_c PBT DSC
PBT	>35	46	-				145.5	≈ 50	
P1700/25	19 - 27	-52	-50	-54	1.32	215	56.3	39	165
P1700/40	11 - 14	-57	-55	-55	0.63	212	71.2	48	164
P1700/55	6 - 7	-58	-	-57	0.76	197	68.2	47	146
P2200/25	27 - 45	-58	-56	-59	0.60	219	54.3	37	169
P2200/40	14 - 18	-59	-	-59	0.67	216	65.8	45	166
P2200/55	7 - 9	-62	-59	-61	0.72	205	64.9	44	159
Pure soft block						T_m PEO	ΔH PEO in J/g		T_c PEO DSC
1700			-69	-63	0.83	-1	64.0		-38 [f]
2200			-69	-63	0.88	2	72.0		-40 [f]

[a] Calculated values based on M_n = 40 kg/mol. [b] Values obtained from tan δ, only lowest T_g's are given. [c] Measured at a frequency of 0.5 Hz. [d] Values obtained from the second heating run. [e] Determined assuming a melting enthalpy of 145.5 J/g for perfectly crystalline PBT [16]. [f] Only observed in the first heating run, indicating the T_g of the PEO block measured in *m*-cresol.

Acknowledgement: The authors acknowledge the fruitful discussions with many colleagues at DSM Research.

[1] Adams, R. K.; Hoeschele, G. K.; Witsiepe, W. K.; "*Thermoplastic Elastomers*", 2nd edition, Holden, G.; Legge, N. R.; Quirk, R.; Schroeder, H. E.; editors; Hanser Publishers, Munich **1996**, p. 191.

[2] van Berkel, R. W. M.; Borggreve, R. J. M.; van der Sluis, C. L.; Werumeus Buning, G. H.; "*Handbook of Thermoplastics*", Olabisi, O., editor; Marcel Dekker Inc., NY **1997**, p. 163.

[3] Miller, J. A; McKenna, J. M.; Pruckmayr, G.; Epperson, J. E.; Cooper, S. L.; *Macromolecules* **1985**, *18*, 1727.

[4] Soliman, M.; Dijkstra, K.; Borggreve, R. J. M.; Wedler, W.; Winter, H. H.; *Makromolekulares Kolloquium*, Freiburg **1998**.

[5] Veenstra, H.; Hoogvliet, R. M.; Norder, B.; Posthuma de Boer, A.; *J. Polym. Sci., B* **1998**, *36*, 1795.

[6] Zhu, L. L.; Wegner, G.; Bandara, U.; *Makromol.Chem.* **1981**, *182*, 3639.

[7] Vallance, M. A.; Cooper, S. L.; *Macromolecules* **1984**, *17*, 1208.

[8] Buck, W. H.; Cella, R. J.; Gladding, E. K.; Wolfe, J. R.; *J. Polym. Sci., Polym. Symp.* **1974**, *48*, 77.

[9] Bandara, U.; Droscher, M.; *Colloid Polym. Sci.* **1983**, *261*, 26.

[10] Briber, R. M.; Thomas, E. L. *Polymer* **1985**, *26*, 8.

[11] Lilaonitkul, A.; Cooper, S. L.; *Rubber Chem. Technol.* **1977**, *50*, 1.

[12] Zhu, L. L.; Wegner, G.; *Makromol. Chem.* **1981**, *182*, 3625.

[13] Cella, R. J.; *J. Polym. Sci., Polym. Symp.* **1973**, *42*, 727.

[14] Castles Stevenson, J.; Cooper, S. L.; *Macromolecules* **1988**, *21*, 1309.

[15] Seymour, R. W.; Overton, J. R; Corley, L. S.; *Macromolecules* **1975**, *8*, 331.

[16] Wegner, G.; Fujii, T.; Meyer, W.; Lieser, G.; *Angew. Makromol. Chem.* **1978**, *74*, 295.

[17] Gabrielse, W.; Soliman, M.; Dijkstra, K.; *Macromolecules* **2001**, *34*, 1685.

[18] Schmalz, H.; Abetz, V.; Lange, R.; Soliman, M.; *Macromolecules* **2001**, *34*, 795.

[19] Schmalz, H.; van Guldener, V.; Wouterse, G.; Lange, R.; Abetz, V.; *Macromolecules* **2002**, *35*, 5491.

[20] Wouterse, G.; van Guldener, V.; Schmalz, H.; Abetz, V.; Lange, R.; *Macromolecules* **2002**, *35*, 6946.

[21] Kricheldorf, H. R.; "*Handbook of Polymer Science*", Marcel Dekker Inc., NY **1992**.

[22] Internal DSM information obtained by modeling experiments.